SUPPORT OF 26M HIGH SAND BACKFILL USING A ROCK PILLAR AND STRUCTURAL PROPS

Dino Sarac and Zhendong Li
Bechtel Australia, Brisbane, Australia. Fluor Corporation, Farnborough, UK (formerly Bechtel)

https://doi.org/10.56295/AGJ6114

ABSTRACT

Excavation of a deep underground station required support of high and narrow sand backfill that was placed by others during earlier construction of an adjacent 26m deep basement. The sand backfill was supported by a complex retaining system including a rock pillar and two levels of props. This paper describes design of the support system, monitoring results, retaining system operation and dismantling of the props.

The design employed a number of design methodologies developed from first principles including application of three methods for calculation of earth pressure from narrow sand backfill, using beam analogy for preliminary calculations of stresses in the rock pillar and of prop force, design criteria for assessment of stresses in the rock pillar and analyses of potential influence of temperature changes on prop forces and the rock pillar stresses. Construction and operation of the retaining system included systems for movement monitoring and prop force monitoring. The paper describes how monitoring results confirmed adequacy of design methodologies and enabled flexible operation of the retaining system when needed, such as more frequent adjustments of prop forces which was required due to higher than assumed degree of prop restraint. Dismantling of the propping system included its modification to suit construction methodology of the Station while monitoring results during that stage further indicated agreement with design assumptions.

1 INTRODUCTION

Construction of the deep underground stations for a transportation network involved vertical excavations to depths between 20m and 40m with a large proportion of the excavations in massive moderately weathered rock not requiring ground support, except in surficial soils and completely weathered rock, or when cavities were encountered. This paper presents a case history of a retaining system that was required due to the excavation proximity to sand backfill of a deep basement.

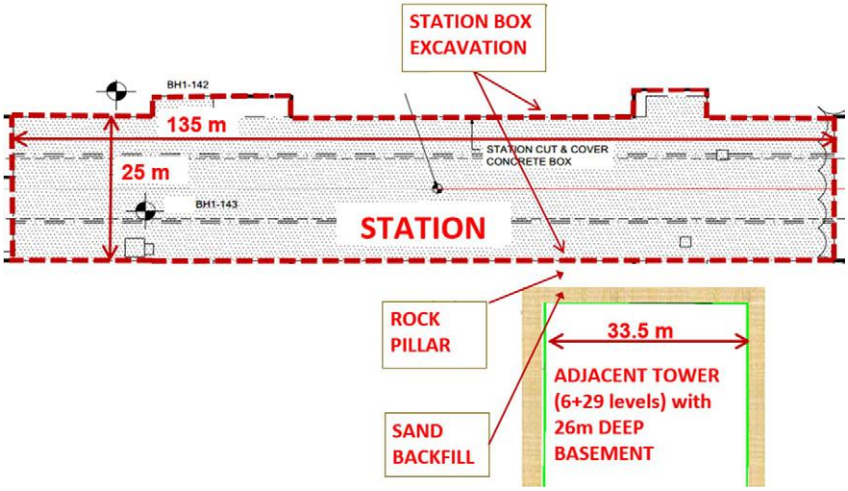

Figure 1: Layout (not to scale) – Station excavation, adjacent tower, sand backfill and rock pillar

Figures 1 and 2 present the excavation layout, location of the adjacent building with 6 basement levels and 29 level tower, sand backfill around the basement and a rock pillar between the excavation of the station main box and the sand. The excavation was 29m deep, depth of the sand backfill was 26m, sand width was 2.8m, and the width of the rock pillar formed by the excavation was 4.3m.

A temporary traffic deck for diversion of a major road extended over the edge of the excavation. The deck was supported on king posts within the station footprint installed as soldier piles before the excavation, and on strip footings and piles in the rock pillar, outside of the excavation. A pressurized 800mm potable water pipe ran all along the excavation and

presented additional risk to the stability. A slotted drainage pipe was installed around the basement before the sand was backfilled; the pipe drained into a pumped sump in the basement.

The adopted retaining system, including 2 levels of props spaced 10m vertically and between 5m and 7m centres horizontally (to avoid clash with the king posts), is shown on sketches and photos in Figures 2, 3 and 4.

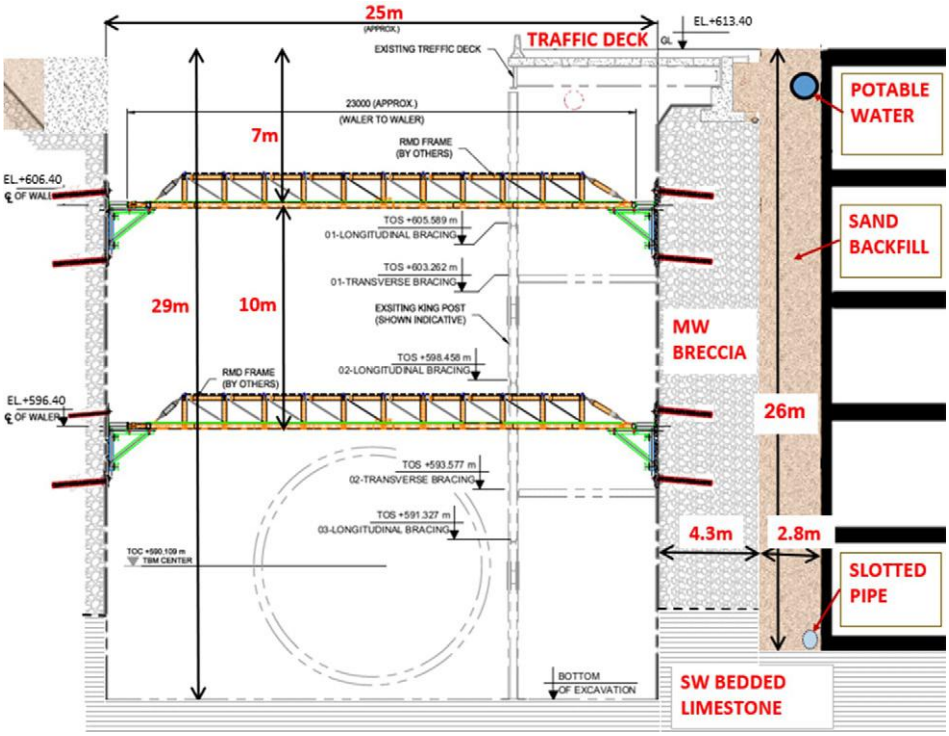

Figure 2: Excavation cross-section (not to scale)

Figure 3: Layout was the same for upper and lower props (not to scale)

2 SUPPORT OF EXCAVATION OPTIONS

At the time when the design was prepared, behaviour of deep excavations along the transportation network was already well understood from other deep excavations in similar geological and geotechnical conditions. Vertical excavations down to depths of about 40m were self-supported, with limited remedial works required only when completely weathered zones or cavities were encountered. A typical deep station excavation is shown in Figure 5. Similar conditions were expected at the site, but the challenge was how to ensure stability of the rock pillar that would be subject to significant horizontal pressures from the backfilled sand.

Figure 4: Left – Excavation about 2m above excavation bottom; Right – base slab already casted

Figure 5: Another station excavation (30 m depth) in similar rock type (Breccia Limestone) and quality

A design of the support of excavation, that was provided by the project's design consultant, required the backfilled sand to be improved by jet grouting with intent to reduce sand gravity pressures on the rock pillar (with no allowance for any additional support of the rock pillar). However, there were major difficulties in implementing this solution including availability of suitably qualified contractors and equipment, high risk of damage to the basement and its water proofing, location of the potable water pipe which could obstruct drilling for the jet grouting, requirement to partially close traffic during the jet grouting and potential to increase horizontal pressures in the sand impacting the basement structure and stability of the rock pillar. Eventually, the jet grouting option was dismissed by project's geotechnical and construction teams due to the risk and unavailability of specialist contractors. At that time, the project's design consultant also provided a recommendation that propping of the rock pillar would be feasible.

Another option used in similar conditions for some shallower excavations was to fully excavate both sand and rock pillar, and expose the basement during construction of the station box. Although this would be much simpler than using props, it could not be implemented because of lack of information about the adjacent tower's structural design. Exposing one basement side would result in an unbalanced load on the tower due to sand pressure from the opposite basement side. It was anticipated that the friction on the sides of the basement and the base would be sufficient to resist the unbalanced force, but full structural assessment of the building structural system and its elements was also required, which was not feasible without detailed knowledge of the building. There was an additional risk of objections by the building owner that could not be quantified. This option would also require changes to traffic diversion plans and redesign of the traffic deck. Overall, this option was also dismissed by the project team.

Finally, it was decided to prop the rock pillar to ensure its stability, to enable uninterrupted traffic flow over the traffic deck, and to protect the adjacent structure. The retaining system design was prepared by the project geotechnical team.

3 GEOTECHNICAL MODEL, ROCK AND SAND PROPERTIES

No boreholes were available through the rock pillar before the excavation. The design relied on 3 boreholes that were drilled at between 60m and 200m distance, and on material properties adopted for geotechnical units that were project-wide, not site specific. Observations of rock exposures during early excavation stages assisted with confirmation of the initial material property assessments, which were further verified by engineering geology mapping as the excavation progressed.

A discussion of broader geological setting and these geological units is outside scope of this paper which is limited to properties relevant for the behaviour of the retaining system at the site. The subsurface conditions in the nearby boreholes indicated 2m to 3m of non-engineered fill overlying Breccia Limestone, to depths between 20m and 23m, over Bedded Limestone.

The Breccia Limestone was mostly cluster dominated, massive without discontinuities, moderately to slightly weathered (MW/SW) and medium strong. Poorly cemented, matrix dominated Breccia, would occur at random in limited extent, and was of low strength. The Bedded Limestone was horizontally bedded, typically without other discontinuities, slightly weathered (SW) and medium strong. From the findings in nearby boreholes, the contact between Breccia and Disturbed Limestone was expected to be close above the bottom of the rock pillar (26 m).

The encountered Breccia is shown in Figure 6. The excavated rock face exposes rock breaker traces and no noticeable fractures. Left image shows weak rock encountered in a very limited zone close to the surface; right image shows markings for anchor drilling to support prop brackets

Figure 6: Breccia Limestone

Groundwater level was measured in the 3 boreholes about 11m below the ground surface during the investigation (about 15m above the bottom of the rock pillar). The slotted drainage pipe at the bottom of the sand backfill (the basement drainage) was expected to fully drain the water and prevent saturation of the sand. To ensure no water pressure on the rock pillar, weep holes were additionally drilled through the rock pillar to drain any water from the sand. Therefore, no water pressure was taken into account for assessment of the rock pillar stability, its stresses and prop forces. No groundwater was encountered during drilling of the drainage holes nor drained through the holes into the excavation during the station construction.

Table 1 presents rock geotechnical properties based on the rock characterization that was carried out project wide by project's geotechnical consultant.

Hoek-Brown strength criterion (1997) was further used to develop and adopt rock mass properties for calculations and modelling in Table 2. Based on the excavation method using the rock breakers, and appearance of excavated surfaces, disturbance was considered to be minimal and Disturbance Factor D, Hoek et al. (2002), was assumed to be zero.

Potential bedding planes in the Bedded Limestone were assumed to be horizontal, have reduced shear strength and no tensile strength. Friction angle of 25° and zero cohesion were adopted according to suggestions by Barton and Choubey (1997) for a smooth rock joint.

For the sand backfill, average properties for loose sand were adopted: unit weight of 17kN/m^3, zero cohesion and friction angle of 30°.

Table 1: Adopted rock geotechnical properties

Parameter	Geotechnical Unit		Comment
	Breccia Limestone	Bedded Limestone	
Unit Weight, γ (kN/m3)	24	24	- median laboratory value(1) - 25th percentile value from gamma logging(1)
Intact Rock UCS, σ_{ci} (MPa)	15	20	- 10th percentile value was 14MPa for Breccia and 23MPa for Bedded Limestone (from UCS laboratory testing(1))
Geological Strength Index, *GSI*	75	75	- Estimated 75 - 90 from rock core and exposures - Adopted the lower bound value
Hoek-Brown Constant, m_i	19	10	- 19(2) is recommended by Hoek (2007) for clastic breccia and limestone, respectively.

Note: (1) Project-wide testing results.
(2) m_i value for breccias extends over a wide range, from values similar to sandstone to values used for fine grained sediments. The value adopted was considered to be representative for cluster dominated material.

Table 2: Rock mass properties

Parameter	Geotechnical Unit	
	Breccia Limestone	Bedded Limestone
Friction Angle, ϕ_m' (°)	44	46
Cohesion, c_m' (kPa)	400	600
Rock Mass UCS, σ_{cm} (MPa)	3.7	5.0
Tensile Strength, σ_{tm} (kPa)	120	300
Deformation Modulus, E_{rm} (MPa)	6000	8000

4 PRESSURE OF LIMITED WIDTH SAND

For the assessment purposes, the sand backfill width of 2.8m was adopted based on findings during drilling of 2 piles for the traffic deck support. The piles, that were 1m diameter, both encountered sand and rock during the drilling. Centres of these piles were at 2.3m distance to the basement; 0.5m was added to account for inability to accurately determine the sand width.

The lateral pressure from the sand backfill was estimated with three methods: initially a closed solution provided by Fan and Fang (2010) was used, followed by a check with limit equilibrium method of slices using SlopeW software, and finally using finite element method (FEM) and PLAXIS software.

4.1 FAN AND FANG (2010) CLOSED-FORM SOLUTION

Fan and Fang (2010) carried out parametric PLAXIS analyses for active pressure of limited width sand on basement retaining walls assuming wall translational movement. They provided a correlation between active pressure coefficient $K_{a(c)}$ for limited width of sand and $K_{a(Coulomb)}$ per Coulomb's conventional theory. The correlation was dependent on wall height/sand depth (H), sand width (b) and angle of inclination of sand zone away from the wall (β). Fan and Fang assumed that the friction angle between the basement wall and the sand was equal to the sand internal friction angle, which was also considered valid for the friction angle between the sand and the rock pillar. Their correlation is presented below and in Figure 7.

$$K_{a(c)}/K_{a(Columb)} = 0.23 + 3.11X - 3.68X^2 + 1.4X^3, where \quad (1)$$

$$0.05 < X < 0.92, \quad (2)$$

$$X = (b + H\tan(90° - \beta))/H \quad (3)$$

The rock pillar sand pressure was a special case of the above equation for vertical sand column, i.e. $\beta = 90°$:

$$X = b/H \tag{4}$$

Active pressures on the rock pillar were calculated using the above approach for the adopted backfill sand width of 2.8 m. The horizontal active pressures on the rock pillar were calculated for the friction angle between the rock pillar and the sand equal to the sand friction angle.

The active pressure horizontal force of 1017kN was obtained by integrating the horizontal active pressures.

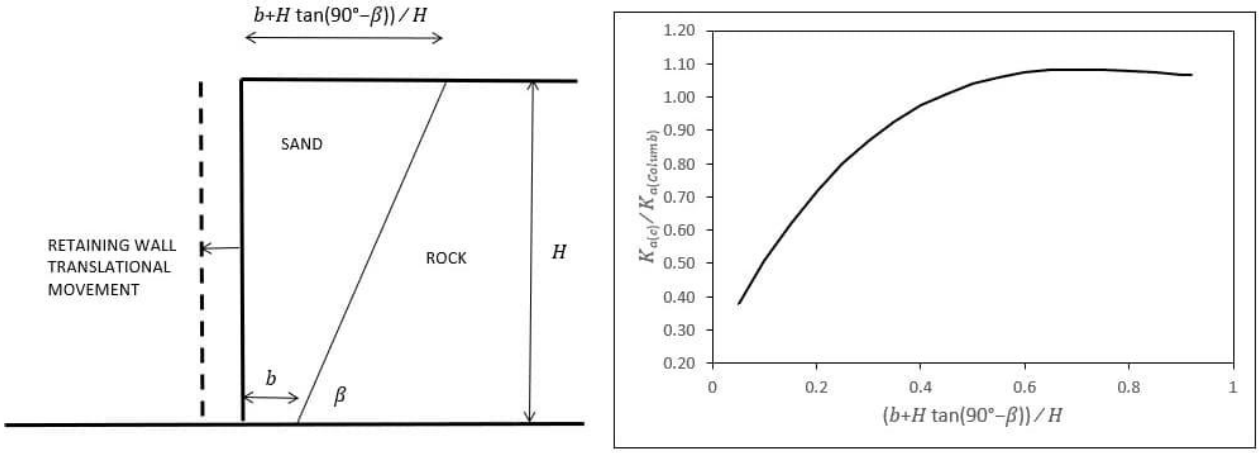

Figure 7: Active pressure coefficient for limited width sand per Fan and Fang (2010)

4.2 LIMIT EQUILIBRIUM METHOD

Bishop's method available in SlopeW program was used to check the active pressure horizontal force. Although method of slices and Bishop's method were not originally developed for calculating active pressure forces, it was considered that obtained values should be similar given that equilibrium of driving and resisting forces must be reached. An online example for SlopeW software by GEO-SLOPE International Ltd suggests a similar use of SlopeW for assessment of active and passive forces. The force was calculated by modelling the sand wedge and the active pressure force as shown in Figure 8, and by varying the force until a factor of safety of 1.0 was obtained. The force was applied at 10.4m above the bottom (about 40% of the wedge height as suggested by Fan and Fang (2010)) and at 30° angle to the horizontal, assuming friction between the rock pillar and sand of 30°. The horizontal component of the calculated force was 935kN/m. This force is about 8% lower than 1017kN obtained from the Fan and Fang solution and indicated a good agreement between the two methods.

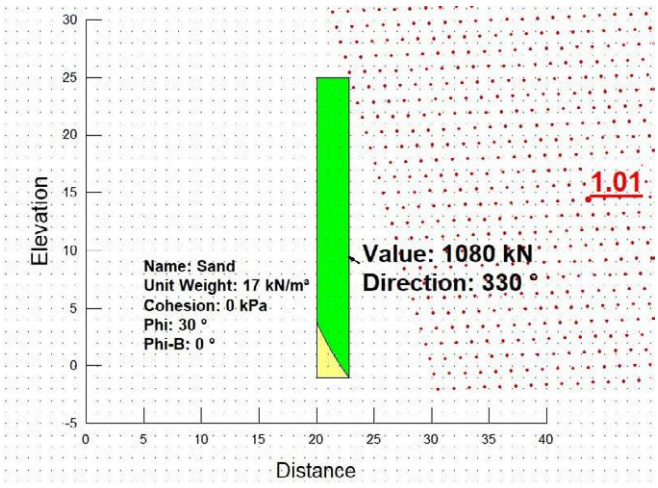

Figure 8: SlopeW model

It should be noted that SlopeW experienced numerical convergence problems for methods of slices that achieve equilibrium of both forces and moments, such as Morgenstern-Price, and that Bishop's method (only moment equilibrium satisfied) had to be used. It is likely that this was caused by a non-conventional shape of the sliding mass. This indicates

that caution should be exercised in using method of slices and SlopeW for limited width sliding mass without having an alternative method to check the results.

4.3 FINITE ELEMENT METHOD

Two-dimensional FEM analysis using PLAXIS was carried out at a later design stage to analyse the retaining system with two prop levels, and to assess temperature effects (FEM model in Figure 9). Sand pressure distribution was obtained by including interface elements and the sand pressure force was obtained by integration of the pressure. The model was run stage by stage to stimulate construction of the adjacent basement and the backfilling of the sand, after which the excavation of the station was simulated.

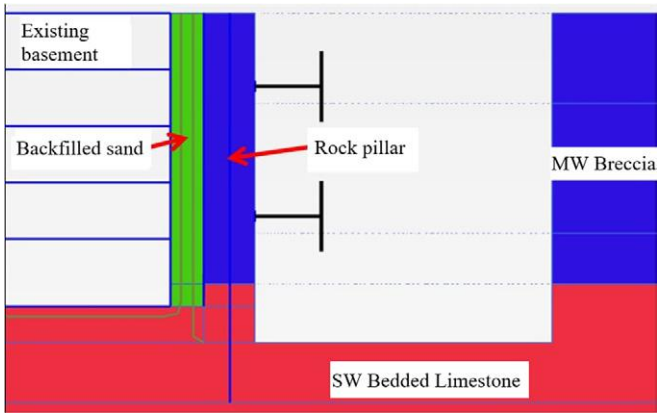

Figure 9: Finite element model

Figure 10 compares horizontal pressure at the rear side of the rock pillar from the FEM model and the pressure profile calculated with earth pressure coefficient $K_{a(c)}$ for limited width sand per Fan and Fang (2010). Coulomb's active pressure is also shown, i.e. full active pressure. The FEM and $K_{a(c)}$ pressure profiles were generally similar except at the top of the rock pillar, where FEM model produced a slightly higher lateral pressure than $K_{a(c)}$. This could be because of the relatively high stiffness of the rock pillar near the surface and incorporation of the propping system, resulting in soil pressures not fully relaxing to the active condition in the FEM model.

From the earth pressure profile in the FEM model, the corresponding total horizontal load was 1180kN/m, 16% higher than 1017kN/m based on the Fan and Fang closed-form solution. Coulomb's active pressure force for the full width sand was 1690 kN/m, 43% higher than the FEM force. If the full active force were used for the propping design, the prop capacity would have to be increased for about 40%, resulting in either larger props or increase in the number of props from 12 to 17 or 18.

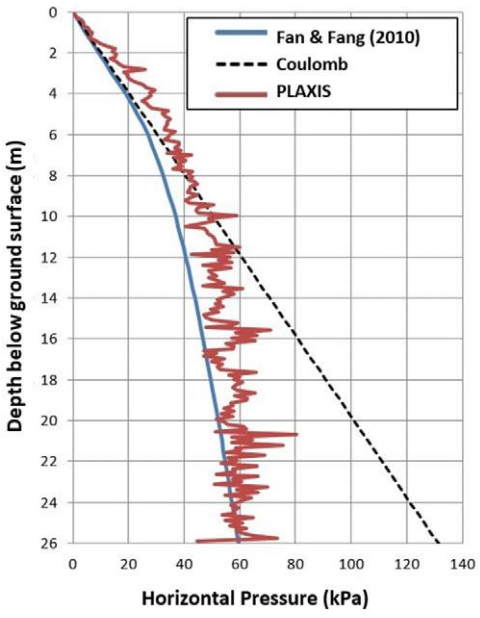

Figure 10: Comparison of sand horizontal pressures

5 ROCK PILLAR PRELIMINARY CHECKS (SIMPLE MODEL)

A preliminary assessment of the feasibility of the retaining system comprised of the rock pillar and props was carried out using an adopted beam analogy – i.e. assuming that the rock pillar is either a cantilever beam or a beam with hinged or fixed end supports, as shown in Figure 11. Soil pressures from Fan and Fang (2010) closed-form solution were then calculated as described under 4.1 and applied on the beam.

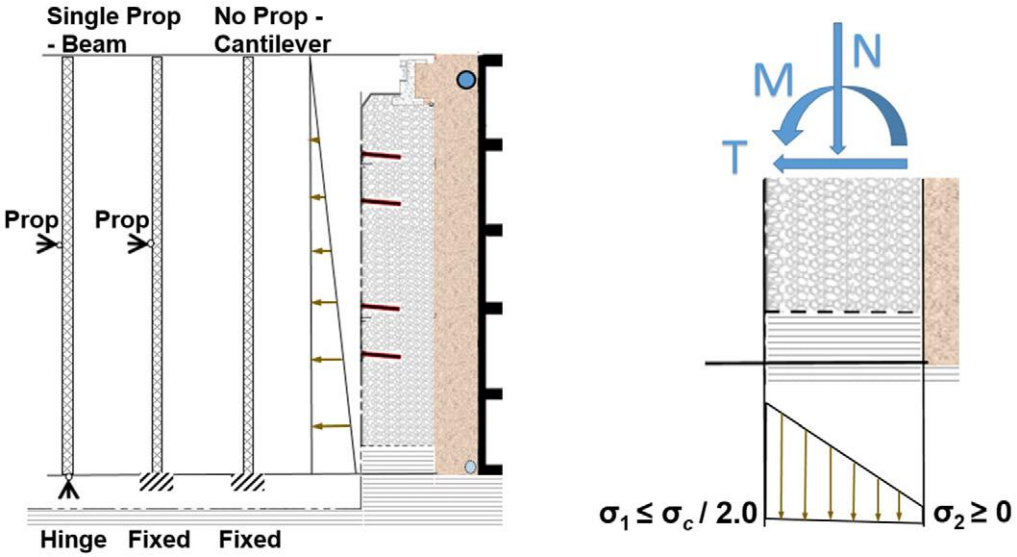

Figure 11: Rock pillar beam analogy and internal forces

A rock pillar without any propping was considered to be a cantilever which had to maintain full fixity at the base. A rock pillar with single prop was modelled as a beam supported at the prop level and at the bottom. The bottom support was expected to exhibit behaviour between hinged and fixed condition and the rock pillar was initially assessed by enveloping those 2 cases. A structural program was run to calculate beam internal forces, i.e. bending moments (M) and shear forces (T). These forces, together with vertical force (N), were used to calculate stresses in the rock mass as indicated on Figure 11. The vertical force was calculated taking into account weights (rock pillar and traffic deck) and vertical component of the sand pressure force. Beam reaction at the prop level was used to roughly estimate the propping force.

Design criteria adopted for these preliminary assessments of the rock pillar are presented in Table 3. Factors of safety were on the conservative side due to the preliminary nature of the assessment and impact on construction progress if a selected option was shown not to be feasible by later more detailed assessments. The design criteria were related to traditional structural and geotechnical approaches:

- Major stress σ_1 (compressive) was compared with rock mass uniaxial compressive strength σ_{cm}, not with intact uniaxial strength, to take into account rock mass effects.
- Factor of safety of 2.0 for the compressive stress was selected to reduce risk of cracking of the rock pillar face and was expected to maintain rock deformations mostly in the elastic range. An analogy with concrete behaviour is that stresses and strains are closely proportional when the stresses do not exceed approximately 50% of the concrete compressive strength (see Darwin et al. 2016).
- No tensile stress was allowed due to concern about ability of rock to develop tensile stresses (for example in case of presence of bedding planes) and from similar approach in design of concrete structures.
- Factor of safety of 2.0 for rock pillar shear was related to conventional factor of safety between 1.5 and 2.0 for sliding of retaining structures.

The cantilever option without any propping was dismissed due to high stresses in the rock pillar – compression of 4.1MPa and tension of 2.7MPa. This was not a surprise, given small width of the rock pillar comparing with the retained height, and that the rock pillar would essentially work as a gravity retaining wall.

For a prop at single level, compressive stresses were acceptable, of the order of 1MPa, but there was tension at the base of the rock pillar of the order of 200 kPa. This initial modelling did not include temperature effects. It was decided to proceed with FEM modelling, re-evaluate single-level prop option, and assess options with props at two levels.

Table 3: Design criteria

Condition	Failure Mode/ Location	Comparison	Criterion/ equation (1)
Rock pillar bending	Compressive stresses and cracking of compressed rock face	Major stress & Hoek-Brown (1997) uniaxial compressive strength of rock mass	$\sigma_1 \leq \sigma_{cm} \div 2.0$ (5) where $\sigma_{cm} = \sigma_{ci} s^a$ (6)
	Cracking due to tension	Minor stress – tension was conservatively not allowed although Hoek-Brown (1997) strength indicated tensile strength σ_t of 120 kPa	$\sigma_2 \geq 0$ (7)
Rock pillar shear	Mass rock (no bedding)	Shear stress in the rock pillar & rock mass shear strength using Hoek-Brown (1997) shear strength parameters	$\tau \leq (c_m' + \sigma_n \tan \varphi_m') / 2$ (8)
	Bedding planes	Shear stress on the bedding plane (bottom of rock pillar) & shear strength of smooth rock joint	$\tau \leq \sigma_n \tan 25°/2,$ (9) where σ_n is normal stress on bedding plane

Note: (1) Rock mass uniaxial compressive strength, cohesion and friction per values in Table 2.

6 TEMPERATURE EFFECTS ON SINGLE LEVEL PROPPING SYSTEM

The FEM model was used for detailed assessment of the retaining system behaviour including addressing influence of temperature changes on the retaining system. Climatic records indicated daily air temperature variation of up to 25ºC, with typical annual range between 5ºC and 50ºC. Local code for bridge design required temperature variation of 60ºC for structural design and that was included in design checks.

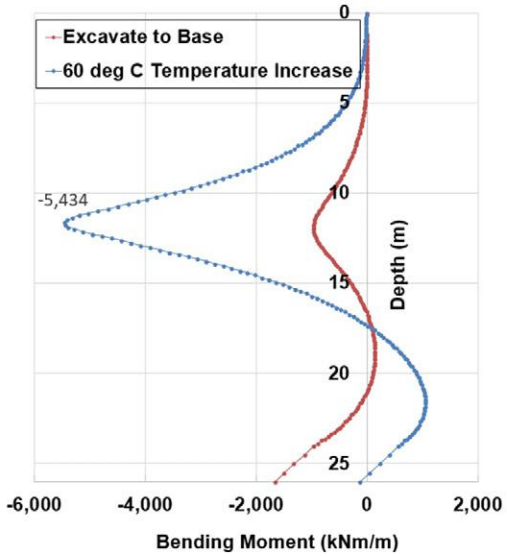

Figure 12: Rock pillar bending moment using beam analogy – single level prop at 11.5m depth

A flexible beam element was incorporated into the FEM model of the rock pillar providing bending moment and shear force distribution which enabled continued use of the beam analogy. Figure 12 presents the rock pillar bending moment for a single prop retaining system, with and without temperature effect (60ºC temperature increase).

For a prop installed at 11.5m depth, force of 670kN/m was calculated, i.e. 4020kN at 6m centres. However, potential daily temperature variation of 25ºC more than doubled this force. This analysis also indicated potentially severe effects of the temperature increase on the rock pillar performance. Major and minor stresses in the rock pillar were 530kPa and 150kPa (both compressive) following the excavation, but 1.9MPa and -1.2MPa (tension) when accounting for a temperature increase of 60 ºC. The results indicated that the large sand pressure force required very stiff props, which could further stress the rock pillar due to temperature forces, potentially resulting in fracturing of the rock and eventual "breaking" of the rock pillar.

To ensure no rock fracturing, a retaining system with 1 prop level would require automated jacks that would continuously adjust the propping force. It was not certain how much time it would require to obtain and install such system at the project location, the costs were relatively high, and there were additional concerns about ability to operate such system continuously over a longer period of time without having experienced personnel available at a short notice if troubleshooting or repairs were needed. This coupled with a general discomfort about having a single prop supporting a rock pillar of 26m height. In the end, a two-level propping option was adopted, which required less stiff props.

7 TWO LEVEL PROPPING SYSTEM

7.1 MODELLING APPROACH

Prop installation levels at 7m and 17m below ground level were selected to avoid large number of potential clashes between props and their hanging system with station permanent floors and traffic deck longitudinal and transversal bracing. There was no opportunity to optimize prop elevations due to these clashes. However, the selected prop levels were generally found to be well suited to the loading conditions.

The same structural truss was selected for both prop levels after preliminary calculation runs and some iterations due to impact of prop stiffness. The safe working load of props was 3720kN and average stiffness of the props was 50280kN/m. A steel thermal expansion coefficient of $12x10^{-6}$mm/mm/ºC was adopted. The total expansion/shrinkage for a free end 25m long steel prop, due to 60ºC temperature change, was 18mm. The load from 60ºC temperature increase assuming fully fixed ends was 5430kN. The props were assumed to have a restraint degree of 40% resulting in temperature load of 0.4x5430kN = 2172kN, or 362kN/m for props spaced at 6m spacing, for the 60ºC temperature increase. The restraint degree of 40% was assumed for design as an average value from a draft of new version of CIRIA C580 Guide (2003) which recommended 50% for stiff retaining walls in stiff soils, and 30% for flexible retaining walls in stiff soils. The 2003 Guide was later superseded by CIRIA C760 Guide (2017) which adopted the same restraint degree range as the draft.

It was decided to model temperature decrease of 40ºC, 30ºC and 20ºC by shortening of the upper prop of 12mm, 9mm and 6mm, respectively. This approach was conservative as it assumed full restraint (100%) of the prop, but it was considered necessary as stresses in the rock pillar could not be directly monitored in operation, and as there was uncertainty about the assumption of 40% prop restraint degree.

Preload force was used to control rock pillar movements and selected depending on prop installation temperature as shown in Table 4 with analyses Cases numbered 1 to 4.

Table 4: Prop Preload for prop installation temperature

Case	Installation Temperature (°C)	Preload (kN)
Case 1	0	100 (nominal)
Case 2	20	1200
Case 3	30	1800
Case 4	40	2000

Effects of temperature increase were investigated in the FEM model by increasing the axial prop force for load calculated using the change temperature, prop stiffness and the restraint factor. Temperature decrease was modelled by reducing the prop axial force to obtain the target shortening of 12mm, 9mm and 6mm. This included some iterations until the target shortening was obtained. The following example details the modelling sequence (an installation temperature of 30°C and a preload force of 1800kN):

1) Over-excavate for the basement construction,
2) Construct the basement,
3) Backfill with sand between the basement wall and basement excavation,
4) Excavate the station box to 8.0m below ground level (bgl.) to install the upper level prop,
5) Install the upper level prop at 7m bgl and preload to 1800kN,
6) Excavate the station box to 18m bgl to install the lower level prop,

7) Install the lower level prop at 17m bgl and preload to 1800kN,

8) Excavate to the final excavation level at 29m bgl,

9.1) Apply the additional axial load in the prop due to 30°C temperature rise by increasing the prop load from soil pressures, P_{soil}, to

$$P = P_{soil} + P_{temperature}\ , \tag{10}$$

where $P_{temperature}$ is 181kN/m from 30°C temperature increase, or

9.2) Continue from stage 8). Simulate temperature decrease of 30°C by reducing the axial loads in props to obtain movement of 9mm at the upper props and loss of prop load equivalent to the restraining force of 30°C in the lower prop.

7.2 ROCK PILLAR MAJOR STRESSES

The stress in the rock pillar was obtained directly from PLAXIS model. Table 4 presents all Cases analysed (4 installation temperatures), rock pillar stresses for excavation to 29m (bgl) and impact of temperature changes. The maximum compressive stresses were at the excavation face, and the tension stresses at rear/sand side, close to the bottom of the rock pillar. A subsequent numerical model run releasing the tension stresses for the case of a horizontal bedding plane presence, which would not be able to transfer tensile stress, did not result in significant increase of compressive stresses movements indicating that performance of the retaining system (rock pillar and struts) was not dependent on the ability of the rock to sustain and transfer tensile stress.

It was concluded that periodic adjustment of the jacking force would be required to control rock pillar stresses, and that these adjustments would depend on prop installation temperature and temperature changes during operation of the retaining system.

Table 5: Summary of temperature analyses

Analyses Case	Rock Pillar Stresses (1)			
	Tension	Factor of Safety	Compression	Factor of Safety
Case 1: Prop installed at 0ºC, preloaded to 100kN				
Excavate to 29m bgl	No tension	N/A	2.6MPa	1.9
60°C temperature increase	No tension	N/A	2.2MPa	2.3
Case 2: Install at 20°C, preloaded to 1200kN				
Excavate to 29m bgl	No tension	N/A	2.1MPa	2.4
Temperature increase for 40°C	No tension	N/A	1.8MPa	2.8
Temperature decrease for 20°C (6mm shortening)	122kPa	2.5	2.6MPa	1.9
Case 3: Prop installed at 30°C, preloaded to 1800kN				
Excavate to 29m bgl	No tension	N/A	2.1MPa	2.4
Temperature increase for 30°C	No tension	N/A	1.9MPa	2.6
Temperature decrease for 30°C (9mm shortening)	96kPa	3.1	2.9MPa	1.7
Case 4: Installed at 40°C, preloaded to 2000kN				
Excavate to 29m bgl	No tension	N/A	2.2MPa	2.3
Temperature increase for 20°C	No tension	N/A	2.1MPa	2.4
Temperature reduction for 40°C (12mm shortening)	218kPa	1.4	3.4MPa	1.5

Note: (1) The maximum stresses are close to the rock pillar bottom within Bedded Limestone.
The rock mass ultimate compressive strength of Bedded Limestone was 5MPa and tensile strength 300kPa, but tensile strength would be zero at bedding planes.

7.3 ROCK PILLAR SHEAR STRESS

Horizontal shear stress for checks of horizontal sliding through the rock pillar was calculated using shear force from the beam analogy for initial assessments, and later using average shear stress on horizontal plane from the FEM model (the 4 Cases from Table 5). The shear stress was compared with Hoek-Brown (1997) shear strength at the upper and lower prop levels, and assuming friction angle of 25º in Bedded Limestone at the bottom of the rock pillar. Minimum factor of safety for the 4 analysed cases varied between 2.8 and 3.4 at all locations, was considered adequate and not critical for performance of the retaining system.

7.4 MOVEMENTS TOWARDS THE EXCAVATION

Table 6 presents maximum movements of the rock pillar towards the excavation for Cases 1 to 4 (as described in Table 5). These results were compared with movement monitoring results in operation as confirmation that the rock pillar behaviour and stresses were within acceptable limits.

Table 6: Maximum rock pillar movements towards excavation (mm)

	Excavation to 26m bgl	Temperature Decrease
Case 1	9(1)	Not applicable
Case 2	5(2)	13(1)
Case 3	2(2)	14(1)
Case 4	1(2)	17(1)

Rock pillar movement pattern: (1) Rotation around bottom
(2) Roughly planar in the top 50%

8 PROPS, PROP FORCES AND FORCE MONITORING

The props had to be sized to resist both soil pressure and temperature load. The allowable axial load of the adopted truss was 3720kN. Each truss comprised six legs as shown in Figure 13.

As mentioned previously, the analyses were carried out assuming a 40% restraint degree. With this approach, the allowable prop load was exceeded only in the lower prop for Case 1 (Table 4), when there was temperature increase of 60ºC. For all other Cases, the maximum load was 3625kN in the upper prop, and 3247kN in the lower prop. Without temperature influence, the maximum load in both props was similar, about 2200kN.

The results indicated that, from perspective of allowable prop load, adjustments of prop forces in operation would not be required if the restraint degree was at about 40%, but would be required if it were higher as the prop loads were close to the allowable load.

Considering overall FEM modelling results, compressive and tension stresses in the rock pillar for cases of temperature decrease, and dependence of the prop axial force on temperature changes and degree of restraint, a jacking system was installed to enable manual control of the prop force. Each of the six truss legs had a jack, and the jacks were connected to a single pump which could apply same pressure (i.e. same force) to each jack (see Figure 13). One of the legs was fitted with a pressure cell for load monitoring, which was connected to a readout unit with a sound alarm set for cases when the allowable load was exceeded.

Shortly after upper level prop installation, a period of no advancement in excavation and variable night temperature was selected to assess degree of prop restraint by comparing theoretical load change from a ’cold’ to a ’warm’ night. The difference between the minimum measured loads during those nights was considered to reflect the temperature influence. Night temperature were selected to avoid any potential influence of sun exposure on steel temperature and prop force. The measured load change was between 60% and 80% of the fully fixed end load, i.e. the restraint degree was 60% to 80% - much higher than originally anticipated in the design.

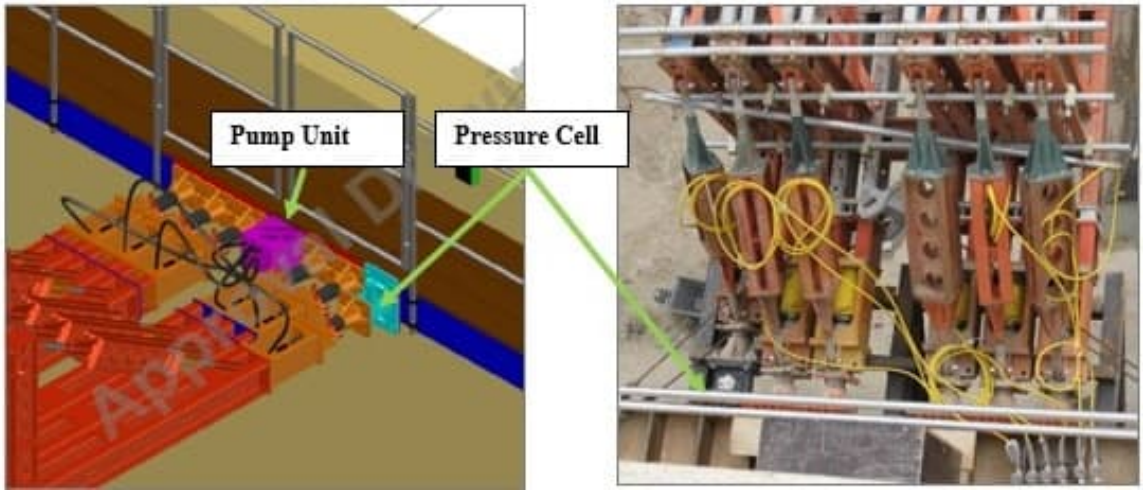

Figure 13: Props, system for load monitoring and adjustment

To account for this behaviour, the load in props was adjusted more frequently than anticipated. In general, once full excavation was reached, the load was maintained between 2100kN (close to the maximum prop load without temperature influence) and 3900kN (about 5% over the allowable prop load).

The load was adjusted 25 times over 80-week operation period, on average every three weeks. At times of abrupt weather changes, the load was adjusted within a few days following a previous adjustment. Figure 14 presents leg load (1/6 of total prop force) of an upper prop and recorded air temperature over the operation period.

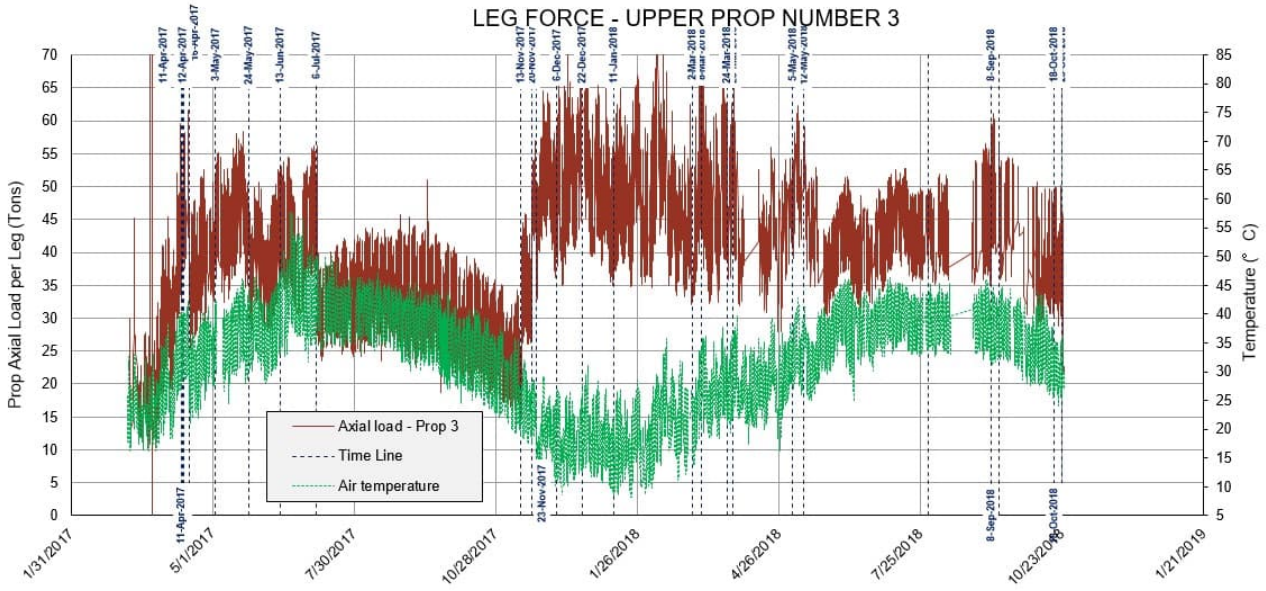

Figure 14: Prop force and air temperature

9 MOVEMENT MONITORING

Excavation movements were monitored using total stations and movement prisms mounted on excavation face. Each station excavation side (135m length x 29 m depth) had four prism rows starting from the top, spaced at 6m to 7m level difference. Each row had eight movement prisms. Some of these prisms were not available due to different obstructions during construction. Vector movements were monitored, but only horizontal movements towards the excavation were significant and are discussed further below. Position of prisms used for monitoring are indicated in Figure 15, and movements of the rock pillar are shown in Figure 16.

The maximum recorded movements of the rock pillar were in the range of 6mm to 7mm before movement monitoring had to be discontinued due to construction obstructions in May 2018. The last major increase in movements, of the order of 1mm, was observed in November 2017 which coincided with completion of the excavation but also with a significant drop in temperature when prop forces were allowed to reduce to about 1500kN. After jacking up of the prop forces, no

further movement was noticeable. These observed movements were somewhat higher than those predicted by the FEM model without temperature effects if the props were prestressed (1mm to 5mm depending on preload force), but lower than movements allowing for shortening of props due to temperature decrease (see Tables 5 and 6). Overall, the recorded movements were of the same order and close to the modelling results, confirming major assumptions of the design approach and that rock pillar stresses were within acceptable limits.

Movements of the excavation opposite side (rock mass) towards the excavation were of the order of 2 to 3mm.

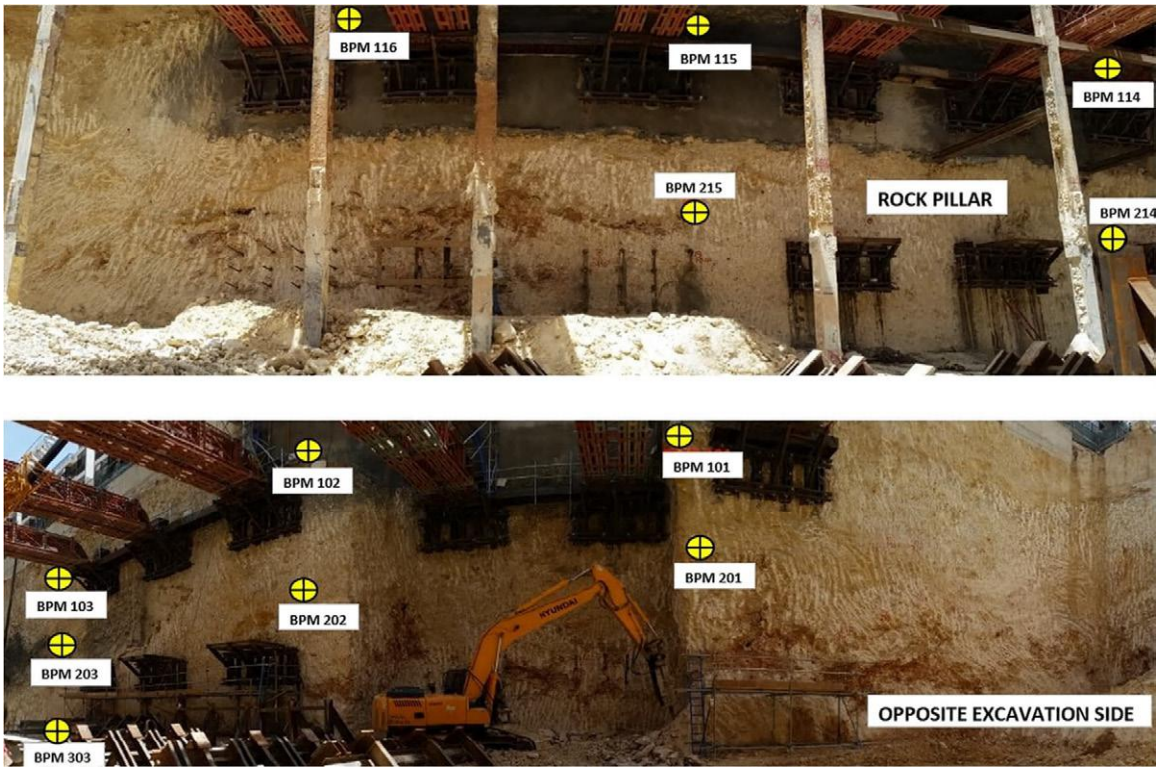

Figure 15: Monitoring prisms – rock pillar (top) and excavation opposite side (bottom) (upper props installed; brackets for support of lower props being installed)

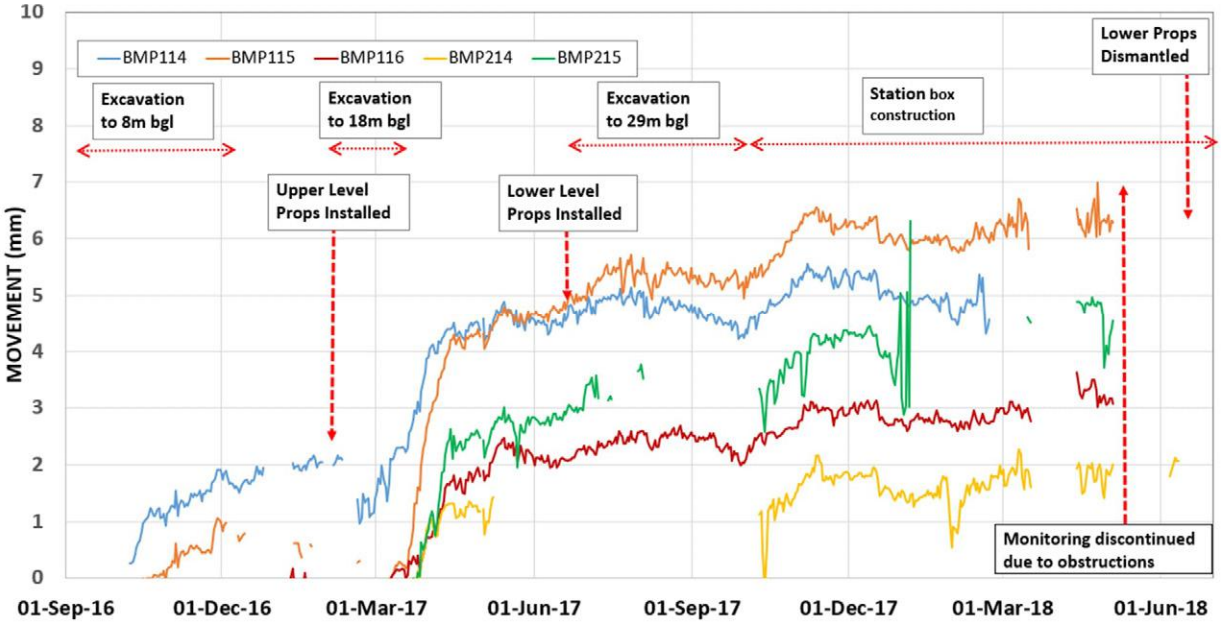

Figure 16: Movement of rock pillar prisms towards the excavation (daily median)

10 DISMANTLING OF THE PROPS

Lower props were dismantled following casting of one of the permanent slabs, which was only 300mm below the props. Unloading was carried out in a gradual manner, starting with 50% load reduction in a single prop which was maintained over 2 days. No increase of loading in the other props was observed either during this initial unloading, nor later during further reduction of load in other props. All the lower props were removed in a smooth process.

The initial plan for removal of the upper props was to cast permanent walls to the underside of the upper props, as a permanent slab was 3.4m below the props. However, this was not considered favourable by the construction team due to requirements for coupling a large number of wall reinforcement bars. Therefore, two trial reductions of prop force were carried out after casting the permanent slab, before the wall was constructed. Each trial consisted of a reduction of the prop force by about 50% in one of the props. However, during both trials, an instantaneous rise of the force was recorded in the remaining props, with the total force increase equal to the force reduction. This was a firm indication that the propping force was needed to control rock pillar behaviour and that removal of the props could lead to large deformations and potential rock pillar failure. Figure 17 includes 2 photographs at the time of the trial force reduction.

To facilitate early prop removal and the proposed construction sequence, an alternative solution with short inclined props against the permanent slab was developed as shown in Figure 17. The short inclined props were installed between a waler beam, which was part of the original system for distribution of loads between the rock pillar and props, and the penetration of the traffic deck column through the permanent slab. As the moment connection between the waler beam and the inclined prop could not be developed due to large forces, a vertical strut against the traffic deck had to be incorporated, utilizing the deck weight for reaction. This system was designed to carry a load equivalent to the prop load. Once the system was fully installed and shimmed to ensure tight connection, gradual reduction of the prop forces was carried out without any observed increase in load of props that were still in operation, and all the prop trusses were dismantled.

Figure 17: Excavation and retaining system during trial force reduction

11 CONCLUSION

The paper has outlined the design, operation, and dismantling of a retaining system consisting of a rock pillar and two levels of props, which successfully supported a 26m high sand column adjacent to critical infrastructure and an active traffic deck. The project addressed significant geotechnical and operational challenges, particularly the need to minimize risk to nearby structures and utilities.

Modelling the actual narrow sand column, validated by three independent methods, resulted in significant savings and a 40% reduction in required propping force compared to conventional approach using full sand width, demonstrating value of a design approach accounting for actual site conditions.

Three methods for assessment of the soil pressure for the narrow sand column were used: the Fan & Fang closed form solution, Bishop's limit equilibrium method of slices, and finite element method modelling. All three produced pressures of the same magnitude. Bishop's method showed satisfactory agreement with the Fan & Fang (2010) solution, differing 8% indicating that method of slices is acceptable for preliminary assessment of active pressures even in special conditions. The FEM results were 16% higher than the close-form solution, likely reflecting influence of retaining system stiffness. For the design of stiff or very stiff retaining systems, the impact of system stiffness on design stresses should therefore be considered in the design.

Assessment of stresses within the rock pillar employed both a beam analogy and FEM modelling, providing a robust basis for engineering the retaining system. The adopted design criteria for the rock pillar - limiting compressive stress to 50%

of the rock mass uniaxial compressive strength, eliminating tensile stress and limiting horizontal shear stress to 50% of the shear strength (rock mass and discontinuities where present) - were found to result in satisfactory pillar performance. Extensive FEM modelling of the influence of the temperature effects on the retaining system provided a good basis for decision making and supported the selection of a manually adjustable jacking system to control propping forces and design uncertainties.

The degree of restraint of 50%, as recommended in CIRIA C760 (2017, Guide for stiff retaining systems in soils), was found to be significantly lower than values observed and not applicable to excavations in rock. Monitoring indicated degrees of restraint of 60% to 80% with this range being recommended where props are supported by rock.

The agreement of movement and force monitoring results with predicted values, and instantaneous redistribution of the propping force into remaining props when the force was reduced in one of the props, demonstrated adequacy of the design methodologies and the FEM approach to capture interaction between the narrow sand column, the rock pillar and the props.

Finally, the use of permanent slab, traffic deck columns, and the deck provided propping action and facilitated early removal of temporary props before station walls reached the underside of the upper props. This was a practical solution adjusted to site conditions and construction staging, highlighting value of having design engineers closely involved in construction.

CRediT authorship contribution statement

Dino Sarac: Conceptualization, Formal analysis, Investigation, Methodology, Supervision, Writing – original draft, Writing - review and editing. **Zhendong Li:** Formal analysis, Investigation, Methodology, Software.

12 REFERENCES

Barton, N., and Choubey, V. (1997). The shear strength of rock joints in theory and practice. *Rock Mechanics,* 1/2, 1977, Vienna, Springer, 1-54.

Darwin, D., Dolan, C. W. and Nilson, A. H. (2016). Design of Concrete Structures. McGraw-Hill Education.

Fan, C. C. and Fang, Y. S. (2010). Numerical solution of active earth pressures on rigid retaining walls built near rock faces. *Computer and Geotechnics,* Vol 37, Issues 7-8, 1023-1029.

Gaba, A. R., Simpson, B., Powrie, W. and Beadman, D.R. (2003). Embedded retaining walls – guidance for economic design. CIRIA C580.

GEOSLOPE International Ltd. Comparison with Active and Passive Earth Pressures. *http://downloads.geo-slope.com/geostudioresources/examples/8/14/SlopeW/Comparison%20with%20active%20and%20passive%20earth%20pressures.pdf*

Hoek, E. (2007). Practical Rock Engineering. *https://www.rocscience.com/assets/resources/learning/hoek/Practical-Rock-Engineering-Full-Text.pdf*

Hoek, E. and Brown, E. T. (1997). Practical estimates of rock mass strength. *International Journal of Rock Mechanics and Mining Sciences,* Vol 34, No 8, 1165-1186.

Hoek, E., Carranza-Torres C. T. and Corkum, B. (2002). Hoek-Brown failure criterion-2002 edition. *Proceedings of the 5th North American Rock Mechanics Symposium*, Toronto, Canada: Vol 1: 267–273.